

Multimerization of *Drosophila* sperm protein Mst77F causes a unique condensed chromatin structure

Nils Kost¹, Sophie Kaiser^{2,†}, Yogesh Ostwal^{1,†}, Dietmar Riedel³, Alexandra Stützer¹, Miroslav Nikolov¹, Christina Rathke², Renate Renkawitz-Pohl² and Wolfgang Fischle^{1,*}

¹Laboratory of Chromatin Biochemistry, Max Planck Institute for Biophysical Chemistry, 37077 Göttingen, Germany,

²Developmental Biology, FB17, Philipps University, 35037 Marburg, Germany and ³Electron Microscopy Group, Max Planck Institute for Biophysical Chemistry, 37077 Göttingen, Germany

Received November 03, 2014; Revised December 11, 2014; Accepted January 08, 2015

ABSTRACT

Despite insights on the cellular level, the molecular details of chromatin reorganization in sperm development, which involves replacement of histone proteins by specialized factors to allow ultra most condensation of the genome, are not well understood. Protamines are dispensable for DNA condensation during *Drosophila* post-meiotic spermatogenesis. Therefore, we analyzed the interaction of Mst77F, another very basic testis-specific protein with chromatin and DNA as well as studied the molecular consequences of such binding. We show that Mst77F on its own causes severe chromatin and DNA aggregation. An intrinsically unstructured domain in the C-terminus of Mst77F binds DNA via electrostatic interaction. This binding results in structural reorganization of the domain, which induces interaction with an N-terminal region of the protein. Via putative cooperative effects Mst77F is induced to multimerize in this state causing DNA aggregation. In agreement, overexpression of Mst77F results in chromatin aggregation in fly sperm. Based on these findings we postulate that Mst77F is crucial for sperm development by giving rise to a unique condensed chromatin structure.

INTRODUCTION

Spermatogenesis encompasses differentiation of male gonadal stem cells into highly functionalized spermatozoa, which are capable to fertilize an oocyte (1). In particular, after meiosis dramatic cellular reorganization takes place to build a motile sperm with highly condensed paternal chromatin. This differentiation process is named spermiogenesis. Transcription is essentially shut down. Original

roundish cells are transformed into slim cells with condensed nuclei and flagella in mammals and needle-shaped nuclei with heavily elongated flagella in flies (2). The DNA undergoes tight condensation, which is caused by structural reorganization of chromatin into unique, mostly non-histone DNA-protein complexes.

Two classes of testis specific, highly positive charged, genome-organizing proteins are thought to accomplish tight DNA packaging in sperm cells independent of histone proteins. In a first step the classical chromatin organization is dissolved and histones are evicted from the DNA. Instead, transition proteins become the short-term organizers of the genome. Subsequently, these proteins are replaced by protamines, the major nuclear proteins found in late spermatids and spermatozoa. Protamines are thought to be linked by disulfide bridges and cause a unique tight chromatin structure by intercalating into DNA (3,4).

While the general framework of sperm chromatin reorganization appears conserved in different species and model systems, such as mice and *Drosophila*, the exact molecular pathways of this stepwise process are still unclear. Numerous histone modifications, such as hyperacetylation of histone H4, ubiquitination of histone H2A and methylation of H3K79, precede histone eviction in mammals and flies and are thought to be necessary but not sufficient for the transition from nucleosomal to protamine-based chromatin (5–8). In mice, histone crotonylation and Lysine 2-hydroxyisobutyrylation characterize the transcriptionally active post-meiotic round spermatids as well as transcriptionally silent elongating spermatids shortly before histone eviction (9,10). Hyperacetylation of histone H4 and methylation of H3K79 are not overlapping with the cytologically detectable level of active RNA Polymerase II in this organism (7). Whereas transition proteins and protamines are indispensable for DNA condensation and fertility in mice (11,12), protamines, their loading factors CAF1-p75 and Tpl94D as well as two transiently expressed chromatin components tHMG-1 and tHMG-2 appear to be non-essential

*To whom correspondence should be addressed. Tel: +49 551 2011340; Fax: +49 551 2011337; Email: wfischl@gwdg.de

†Authors S. Kaiser and Y. Ostwal contributed equally to the paper.

in *Drosophila* (2,13–15). In their absence DNA condensation is largely normal and mutant male flies are fertile. Obviously, other factors are essential for genome reorganization in this organism.

The testis-specific protein, Mst77F is crucial for male fly fertility (16,17). Its nuclear expression coincides with the removal of histone proteins from chromatin and immunocytological studies in developing spermatids have shown that Mst77F globally colocalizes with DNA and microtubules responsible for nuclear shaping (17). In contrast to transition proteins, Mst77F is retained in sperm as a nuclear component in distinct areas of differentiated spermatozoa (17). However, it is unclear whether Mst77F has a causal role in histone removal or chromatin compaction.

Mst77F is related to HILS1 of mammals (homology of 41%, see Supplementary Figure S1), which has been suggested to be a linker histone variant implicated in chromatin remodeling during spermiogenesis (18,19). In mice, HILS1 is expressed in spermatids and forms part of histone-based chromatin. It is lost later than histones but is unlike *Drosophila* Mst77F not present in mature sperm (17,19). In *Saccharomyces cerevisiae*, the nucleus is compacted 10-fold in spores, which requires the linker histone Hho1 (20).

Due to the distant sequence similarity with linker histones of the H1 type (Supplementary Figure S1) it has been proposed that Mst77F has DNA-associated functions (21). As so-called architectural proteins linker histones act as major components of somatic chromatin mediating higher order folding via binding to nucleosomal DNA (22). Histone H1 proteins are characterized by a tripartite domain organization (23,24) (Figure 1A). A globular winged-helix fold that specifically binds the nucleosome at the dyad axis is flanked by short N-terminal and long C-terminal unstructured domains. These regions unspecifically interact with DNA through their high content of positively charged amino acids (23,25). Whether Mst77F functions analogous to linker histones or has different properties is unclear, since its molecular working mechanism and cellular function have not been investigated.

Here, we examined a putative role of Mst77F as DNA/chromatin architectural protein. We analyzed structural effects on chromatin *in vitro* and *in vivo* and deduced the consequences of elevated levels of Mst77F in spermatids and sperm. Furthermore, we conducted biochemical, biophysical as well as single molecule experiments to analyze its interaction with DNA. Our results show that Mst77F binds DNA through an intrinsically unstructured C-terminal domain (CTD) via unspecific electrostatic interactions with the sugar-phosphate backbone of the nucleic acid. However, in contrast to linker histones, Mst77F is induced to multimerize upon binding of DNA. This process involves the N-terminal region, which contains a putative coiled coil domain. The result of these events is major condensation of DNA *in vitro* and aberrant chromatin aggregation *in vivo*. We propose that cooperativity between intra- and intermolecular interaction of Mst77F and its DNA-binding properties results in a novel mode of tight DNA packing that is involved in chromatin reorganization in spermiogenesis.

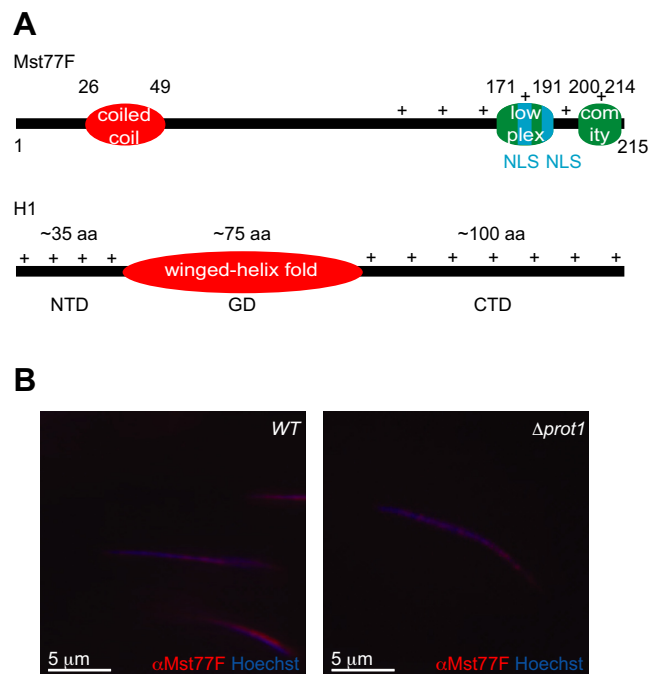


Figure 1. Mst77F chromatin association is independent of protamines. (A) Top: domain architecture of Mst77F according to SMART prediction: N-terminal coiled coil motif (red) as a possible protein-protein interaction module and C-terminal low compositional complexity regions (green) with undefined structure and function. Two putative nuclear localization signals (NLS) in the C-terminal domain are indicated. Numbers indicate boundaries of different regions. The C-terminal part of the protein is enriched in positively charged amino acids (lysine, arginine). Bottom: generic domain architecture of a linker histone H1 protein. The N-terminal (NTD) and C-terminal (CTD) domains are considered unstructured and are enriched in positively charged amino acids. The globular domain (GD) consists of a winged-helix fold. (B) Expression of Mst77F in individualized *Drosophila* sperm was analyzed by anti-Mst77F antibody staining in WT and $\Delta prot1$ mutant flies. Hoechst staining marks the DNA.

MATERIALS AND METHODS

Reagents

Details of plasmids, antibodies, DNA templates and recombinant chromatin can be found in Supplementary Materials and Methods.

Protein expression and purification

Mst77F and hH1.4 proteins were expressed in *Escherichia coli* BL21RIL (NEB). Bacterial cells were lysed at 4°C in 20 mM HEPES-NaOH pH = 7.4, 1 M NaCl, 50 mM imidazole, 1 mM β -mercaptoethanol, 1 mM PMSF using an EmulsiFlex-C5 cell disrupter (Avestin). Proteins were purified on HisPur Cobalt Resin (Thermo Scientific), dialyzed against storage buffer (50 mM imidazole pH = 6.4, 300 mM NaCl, 10% (v/v) glycerol, 1 mM β -mercaptoethanol) and stored at -80°C .

Micrococcal nuclease digestion

MNase digests of isolated nuclei were done as described (26). The procedure was further adapted to recombinant

mono- and oligonucleosomes as described in Supplementary Materials and Methods.

Fluorescence polarization (FP)

FP assays were essentially carried out and analyzed as described using FP buffer (10 mM triethanolamine-HCl pH = 7.4, 150 mM NaCl) (27).

Protein cross-linking

Cross-linking of Mst77F was carried out in 10 mM triethanolamine-HCl pH = 7.4, 150 mM NaCl, 1 mM DTT at a concentration of 20 μ M in 10 μ l reaction volume. A 2434 bp DNA fragment isolated from pUC18 was titrated to the protein in 2-fold increments from 0.5 to 8 μ g/reaction. Reactions were allowed to equilibrate for 30 min at room temperature (RT) prior to addition of BS³ (Bis[sulfosuccinimidyl]suberate) (Thermo Scientific) to a final concentration of 400 μ M. After 30 min reactions were quenched by addition of 100 mM Tris-HCl pH = 7.4.

Centrifugation fractionation assay

Assays were essentially carried out as described with slight modifications (28). Details can be found in Supplementary Materials and Methods.

Analytical ultra centrifugation

Analysis was carried out at OD₂₈₀ = 0.8 of recombinant Mst77F in 400 μ l triethanolamine-HCl pH = 7.4, 150 mM NaCl, 1 mM β -mercaptoethanol with samples equilibrated to 20°C for 1 h. During runs (35,000 revolutions per minute), scans (200 total) were continuously acquired. Data analysis was performed using the SEDFIT software and a partial specific volume of Mst77F calculated from the amino acid composition (SEDNTERP) (29). Generally, after positioning the meniscus and the bottom, a simplex fit for the meniscus position was performed at a resolution of 50–100. The frictional ratio was fitted with the simplex algorithm. The initial fits were further refined by the simulated annealing algorithm until the root mean square deviation converged at a minimum.

Atomic force microscopy

DNA and proteins were extensively dialyzed against sample deposition buffer (10 mM triethanolamine-HCl pH = 7.4, 150 mM NaCl, 1 mM MgCl₂ and 1 mM DTT). For analysis of 2434 bp DNA, 3.71 fmol (0.3 ng/ μ l) DNA were incubated with varying amounts of Mst77F and control proteins (4-, 20- and 100-fold molar excess of protein over DNA) in a total volume of 20 μ l at RT for 30 min. Samples were deposited on mica (Plano), incubated for 10 min and washed with 2 ml of ddH₂O. For analysis of 12 bp random DNA, 0.04 μ M were incubated with 0.04 or 0.64 μ M Mst77F in a final volume of 50 μ l. After 1:10 dilution in deposition buffer aliquots of 20 μ l were pipetted onto mica and processed as before. Prior to imaging samples were dried for 20 min in a stream of filtered compressed air. Images of

the different protein-DNA complexes were recorded on a Nanoscope V instrument (Bruker) using tapping mode in air and a NSC15/no Al cantilever (μ Masch, resonance frequency of 325 kHz and force constant of 40 N/m). Scans were recorded at a rate of 0.996 Hz with a resolution of 512 \times 512 pixels. Post-imaging flattening of data files was conducted with the Nanoscope software.

Circular dichroism (CD)

Protein samples were dialyzed into 10 mM triethanolamine-HCl pH = 7.4, 150 mM sodium fluoride and concentrated to 30 μ M. CD spectra (260 to 180 nm, step size of 0.5 nm, bandwidth of 1 nm, dwell-time per data point of 3 s) were recorded on a ChiraScan spectrometer in terms of ellipticity Θ at 20°C in a 1 mm Quartz CD cell (Hellma). Curves of replicate measurements were smoothened using the instrument software. Data points were exported and plotted with the Kaleidagraph software.

Electrophoretic mobility shift assay (EMSA)

20 nM to 1.28 μ M Mst77F were added to 250 ng nucleosome core particles in EMSA buffer (10 mM HEPES-NaOH pH = 7.4, 50 mM KCl, 0.25 mg/ml bovine serum albumin, 5 mM DTT, 5% (v/v) glycerol) to a final volume of 15 μ l. Reactions were incubated at RT for 20 min and subsequently loaded onto 5% 0.5 \times TBE – polyacrylamide gel electrophoresis (PAGE) gels. Gels were run at constant 100 V in the cold room for 90 min. DNA was stained with 0.5 μ g/ml EtBr in running buffer for 20 min and visualized on a Biorad UV imager.

Ectopic expression of Mst77F-eGFP

For ectopic expression in testes we used previously established transgenic *Mst77F-eGFP* flies (16). Mst77F deletion constructs were generated by polymerase chain reaction (PCR) using genomic DNA from wild-type (WT) flies and the following primers containing different restriction sites: *Mst77F Δ 20C-eGFP*, *Mst77F-Pr-Kpn* (5' GATGGTACCGCGTTACTCAG 3') and *Mst77F Δ 20C-Spe* (5' GAT-ACTAGTGCCGCATTCCATC 3'); *Mst77F Δ 40C+NLS-eGFP*, *Mst77F-Pr-Kpn* and *MstF Δ 40CNLS-Spe* (5' GAT-ACTAGTCTTCCGGGGTCGCTTCGGTTTGCCG 3'); *Mst77F Δ 100N-eGFP*, *Mst77F-Pr-Kpn* and *Mst77F-Pr-SacII2* (5' GATCCGCGGTTTGCAACCAATC 3') to amplify the regulatory region and *Mst77F Δ 100NSacII* (5' GATCCGCGGATGCATGTAGAGCCC 3') and *Mst77FStopBamHI* (5' GATGGATCCTTACATCGAGCACTTG 3') to amplify the shortened open reading frame. The PCR products were restriction digested with *Kpn I* and *Spe I*, *Kpn I* and *Sac II*, or *Sac II* and *BamHI* and cloned into pCR[®]II-TOPO[®] (Invitrogen). cDNAs were subcloned into the germ line transformation vector *pChab Δ Sal Δ LacZ*, which supplies an in-frame C-terminal *eGFP* and the 3'UTR from SV40 (30). Independent transgenic *Drosophila* lines were established by injection of DNA as described (31). At least five independent strains were analyzed.

Adult testes were dissected. eGFP and Hoechst signals as well as immunofluorescence staining were examined (Zeiss

Axioplan2). Images were individually recorded and processed (Adobe Photoshop CS2/CS5). Anti-Mst77F and anti-histone staining was performed as described previously. The Mst77F-eGFP and protamine-deficient strains have already been reported (17). Sterility tests were performed at least 10 times per genotype.

RESULTS

Mst77F has features similar to but also distinct from linker histones

To clarify a possible role of the Mst77F protein in DNA reorganization during post-meiotic differentiation processes of *Drosophila* spermiogenesis, we first performed bioinformatic analysis of the protein sequence to identify conserved regions corresponding to putative functional domains. Motif prediction analyses of Mst77F did not reveal a conserved winged-helix fold characteristic of linker histones, including HILS1 but projected a coiled coil domain in the first half of the protein (Figure 1A). Similar to histone H1 proteins, a short N-terminal region and the vast majority of the C-terminus (second half of the primary sequence) were predicted to be in random coil conformation. The later included regions of low compositional complexity, nuclear localization signals (NLS) and a very high content of basic amino acids (30% of residues in the CTD are Arg or Lys) (Supplementary Figure S1).

Mst77F is deposited to the sperm chromatin independent of protamines

In *Drosophila*, protamines A and B as well as Mst77F localize to sperm chromatin (16,17). We asked if the localization of Mst77F in mature sperm is dependent on the presence of protamines. We previously obtained evidence that Mst77F is synthesized independent of protamines and is distributed in distinct speckles in sperm chromatin (17). In mature sperm of *wild-type* (WT) and $\Delta prot1$ males no obvious difference in Mst77F distribution was seen (Figure 1B).

Mst77F induces chromatin compaction *in vitro*

To analyze whether Mst77F has autonomous effects on chromatin or requires cellular cofactors, we set up *in vitro* systems. First, we analyzed interaction of Mst77F with recombinant oligonucleosomal arrays reconstituted on the 12 × 200 bp × 601 DNA sequence (Figure 2A) (32). In coprecipitation experiments we detected association of the protein with chromatin that could not be saturated at 4-fold molar excess of the protein compared to histone octamers. We also noted that binding of increasing amounts of Mst77F did not cause eviction of any core histone from the chromatin fiber. Next, we analyzed the consequence of Mst77F binding for chromatin conformation. Addition of Mst77F was sufficient to impair MNase digestion of recombinant oligonucleosomal arrays (Figure 2B). While the effect was weaker compared to linker histone hH1.4, imaging of the oligonucleosomal arrays by atomic force microscopy clearly indicated significant chromatin compaction and aggregation induced by Mst77F (Figure 2C).

We then asked whether Mst77F could also affect cellular chromatin. Since overexpression of the protein in S2 cells induced apoptosis (data not shown), we resorted to an *ex vivo* system. As Figure 2D shows, addition of Mst77F to intact nuclei isolated from S2 cells was sufficient to induce chromatin compaction, which was reflected in resistance to MNase digestion. The effect in this assay was comparable to that of linker histone hH1.4. Overall, the results implied that Mst77F has direct effects on chromatin conformation reminiscent of architectural proteins.

Mst77F functions differently from linker histones

Since Mst77F bound DNA simultaneous with core histones and also had chromatin effects reminiscent of linker histones, we tested whether it could function as a specialized *Drosophila* testis restricted H1. Within the nucleosome linker histones occupy the entry/exit point of DNA on the histone octamer thereby protecting linker DNA (22,23). We performed MNase digestion assays of nucleosome core particles reconstituted on 187 bp × 601 DNA in the presence of Mst77F or hH1.4 (Figure 2E). Whereas the linker histone clearly protected linker DNA from degradation thereby slowing down transition of nucleosomes to 147 bp nucleosome core particles, Mst77F failed to do so. Compared to control mono-nucleosomes increased amounts of intermediate length DNA could be observed in the reactions containing Mst77F. These might be due to association of the protein with more distal regions of linker DNA, which might impede digest by MNase. However, in gel shift experiments we found Mst77F capable of associating with DNA on the surface of nucleosome core particles (Supplementary Figure S2). We deduced that binding to free linker DNA is preferred in the context of nucleosomes due to higher negative charge density. In comparison, the charge of DNA that is wrapped around the histone octamer in the nucleosome core particle is more shielded.

Association of Mst77F with recombinant chromatin different from linker histones, the distinct spatio-temporal expression pattern as well as the distinct domain architecture implied that Mst77F does not act as an H1 homolog. While a pivotal role of the globular winged-helix domain of linker histones is nucleosome targeting (24,33), the function of the Mst77F putative coiled coil domain is unclear. To understand the functional role of Mst77F and especially its N-terminal region during post-meiotic spermatid maturation, we analyzed the complexes the factor forms with DNA in more detail.

Mst77F binds DNA via its CTD

We prepared a series of deletion mutants for *in vitro* binding studies to explore Mst77F interaction with DNA (Figure 3A, Supplementary Figures S1 and S3A). These were analyzed in qualitative pull-down experiments (Supplementary Figure S3B) and quantitative FP binding assays (Figure 3B–E) with short, random sequence 12 bp DNA. The WT protein showed robust binding to the double-stranded oligonucleotide template with a K_d of $0.09 \pm 0.02 \mu\text{M}$. This interaction was dependent on the CTD as sequential deletion of residues from the C-terminus (Mst77F $\Delta 20\text{C}$,

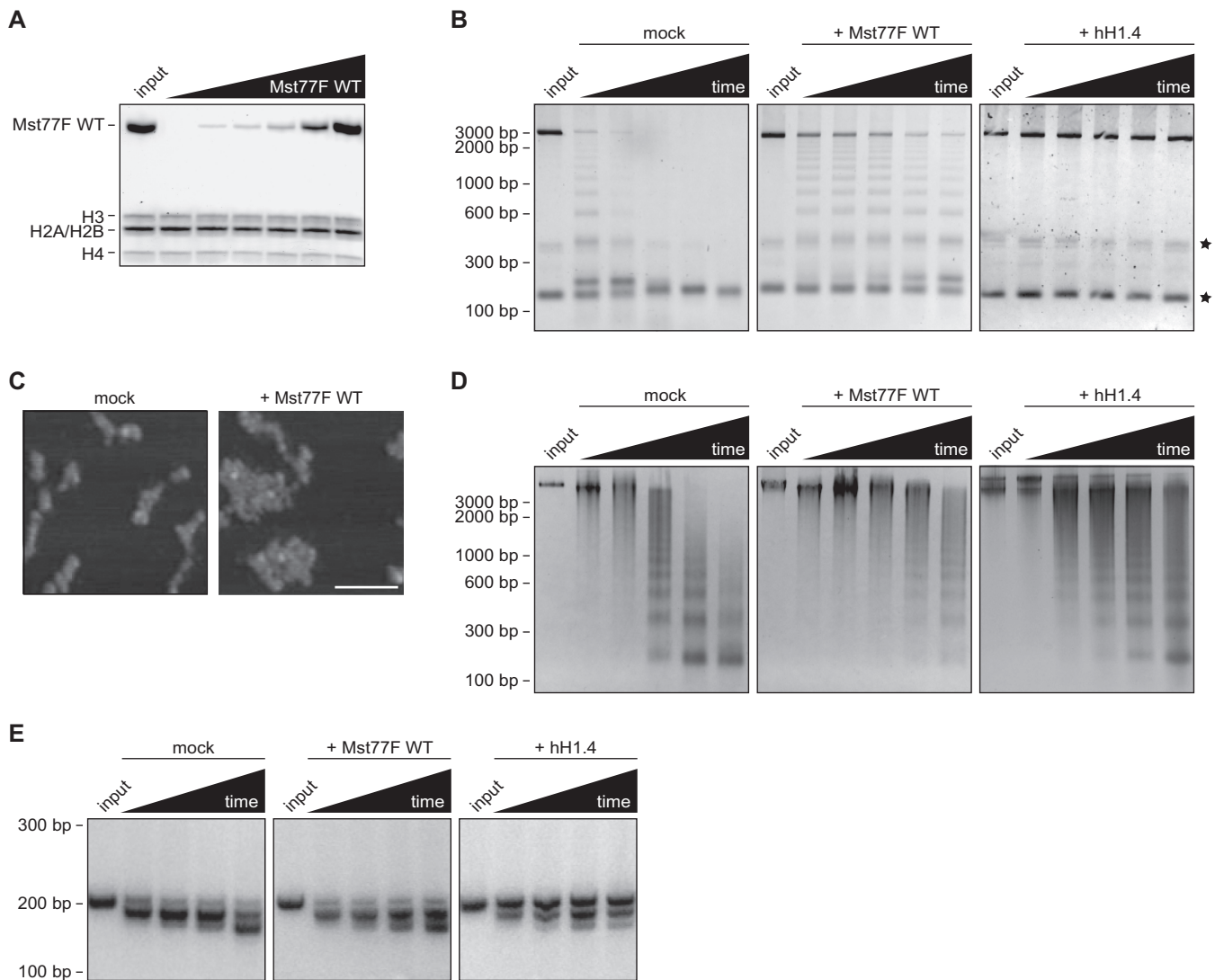


Figure 2. Recombinant Mst77F binds chromatin and induces aggregation. (A) 12 × 200 bp x 601 DNA-based oligonucleosomal arrays were incubated with increasing amounts of Mst77F (none, 0.23–3.71 molar excess over histone octamers). Clustering of protein-chromatin complexes was triggered by addition of $MgCl_2$. Complexes were recovered by centrifugation and analyzed by sodium dodecyl sulphate-PAGE (SDS-PAGE) stained with Coomassie Blue. Input, chromatin and Mst77F (highest concentration) before precipitation. (B) Recombinant 12-mer oligonucleosomal arrays were incubated with the indicated proteins and digested with MNase. DNA was isolated and analyzed on a 1% TBE-agarose gel that was stained with EtBr. Mock, no protein added; input, no MNase added; time, digest for 1, 2, 4 or 8 min. The asterisks mark major (bottom) and minor (top) scavenger DNA species used in the chromatin assembly procedure. (C) AFM images of 12-mer oligonucleosomal arrays in absence (mock) or presence of Mst77F (4-fold molar excess over DNA). Images were recorded in tapping mode; scale bar represents 100 nm. (D) The indicated recombinant proteins were added to nuclei isolated from S2 cells. MNase digest was performed and analyzed as in (B). Mock, no exogenous protein added. (E) MNase digest of 187 bp x 601 DNA-based nucleosome core particles in presence of the indicated recombinant proteins. Mock, no protein added; input, no MNase added; time, digest for 1, 2, 4 or 8 min. DNA was extracted and analyzed on a 5% TBE-PAGE gel that was stained with EtBr.

Mst77F $\Delta 40C$, Mst77F $\Delta 60C$) resulted in successive loss of binding affinity. Consequentially, the Mst77F $\Delta 110C$ mutant displayed no interaction. Deletion of the N-terminus (Mst77F $\Delta 100N$), in contrast, had no effect on Mst77F binding to DNA. Since the CTD does not contain any structural motifs but has a high density of positive charge, we reasoned that unspecific electrostatic interaction is the predominant mechanism of DNA binding.

To test this idea, we first analyzed a mutant Mst77F protein where the sequence of the CTD was randomized (Mst77F CTD*). In FP experiments with the random sequence 12 bp DNA this protein displayed binding strength

that was at $K_d = 0.06 \pm 0.01 \mu M$ even slightly enhanced compared to the WT factor (Figure 3B and C). Next, we measured the interaction of Mst77F WT with DNA at different salt concentrations. As Figure 3B and D show, DNA binding was severely reduced when going from 20 ($K_d = 0.11 \pm 0.05 \mu M$) to 450 mM NaCl ($K_d = 17.9 \pm 7.5 \mu M$). Finally, we analyzed DNA templates of different properties. Poly-GC and poly-AT 12 bp DNA showed at $K_d = 0.17 \pm 0.06 \mu M$ and $K_d = 0.07 \pm 0.03 \mu M$, respectively, binding strength comparable to the randomly chosen sequence. Incubation of DNA with ethidium bromide that unwinds B-DNA also had no effect. Finally, interaction with a single-

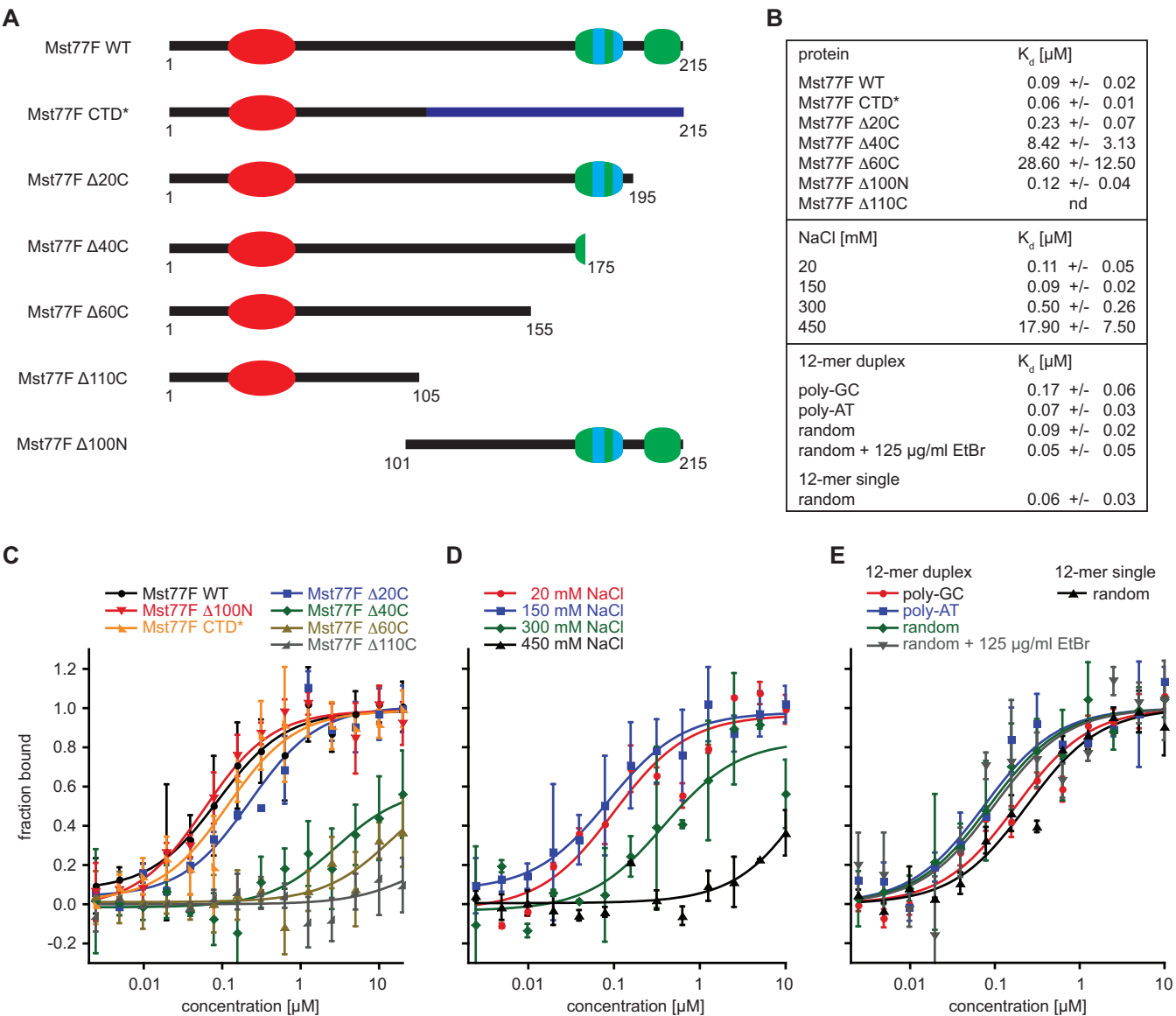


Figure 3. Mst77F binds DNA electrostatically. (A) Schematic representation of different mutant Mst77F proteins used in this study. Purity of recombinant proteins is shown in Supplementary Figure S3A. For analysis of transgenic flies an artificial NLS was added to Mst77F Δ 40C-eGFP and Mst77F Δ 60C-eGFP. (B–E) Analysis of binding of Mst77F WT and mutant proteins to different DNA templates and under different conditions using FP. Average signals of at least three independent experiments are plotted. Error bars represent standard deviation. (B) Dissociation constants (K_d in micromolar concentration) derived from the equilibrium binding analyses. (C) Binding curves of interaction of the indicated Mst77F proteins with 12 bp random DNA. (D) Binding curves of interaction of Mst77F WT with 12 bp random DNA at the indicated salt concentrations. (E) Binding curves of interaction of Mst77F WT with the indicated DNA probes.

stranded template was at $K_d = 0.06 \pm 0.03 \mu\text{M}$ similar to binding to double-stranded DNA (Figure 3B and E). Based on these experiments we concluded that the CTD is necessary and sufficient for electrostatically driven, unspecific interaction of Mst77F with DNA.

Mst77F aggregates DNA

Based on the direct binding of Mst77F to DNA as well as the observed condensing and aggregating effects on chromatin, we tested whether Mst77F has a direct impact on DNA. Precipitation analysis was performed according to

the scheme in Figure 4A with constant amounts of the random sequence 12 bp DNA used for binding studies and increasing Mst77F WT ($pI = 9.86$) or Mst77F Δ 100N ($pI = 10.57$) protein concentrations. hH1.4 ($pI = 11.03$) and the similarly positively charged xPR-Set7 ($pI = 9.52$) served as control. In this assay, Mst77F WT protein efficiently precipitated all DNA from solution at $1.28 \mu\text{M}$ protein concentration ($IC_{50} = 0.5 \mu\text{M}$), suggesting the formation of massive protein-DNA complexes. In contrast, the Mst77F Δ 100N mutant protein, but also hH1.4 did only induce very limited DNA aggregation in the tested concentration range. xPP-Set7 had no effect (Figure 4B).

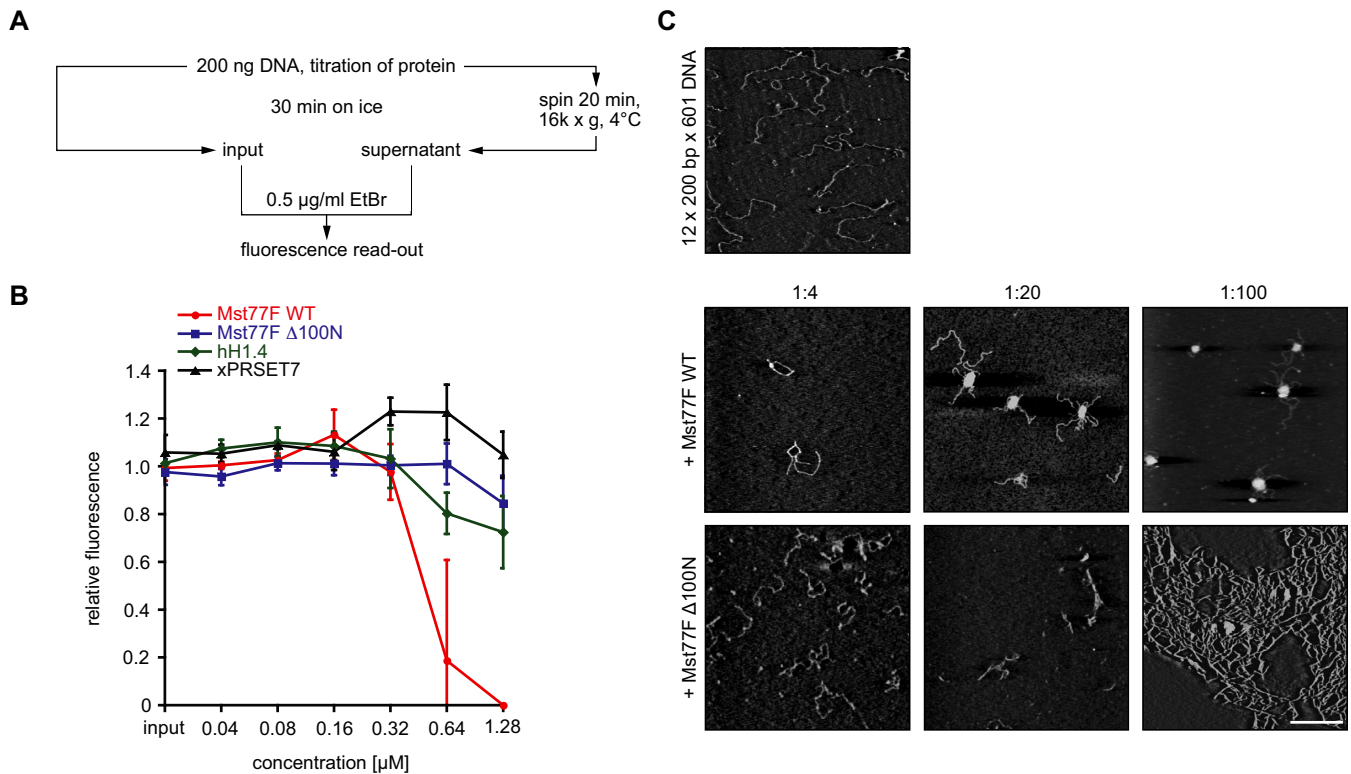


Figure 4. Mst77F causes DNA aggregation. (A) Scheme of centrifugation-fractionation experiment. (B) 12 bp DNA was incubated with the indicated proteins (0.04–1.28 µM in 2-fold increments). Average ratios of DNA in the output sample (i.e. supernatant after centrifugation) to total DNA (input sample) of three independent experiments are plotted. Error bars represent standard deviation. (C) Mst77F WT and Mst77F Δ100N were complexed with 2434 bp DNA at 4-, 20- and 100-fold molar excess of the protein over DNA. AFM images were recorded in tapping mode and flattened by the instrument software. Scale bar represents 50 nm.

To corroborate the data of the hydrodynamic analysis, we analyzed Mst77F WT and Mst77F Δ100N complexes with the 12 bp DNA by atomic force microscopy (Supplementary Figure S4A). In good agreement with the hydrodynamic assay, the WT protein aggregated the DNA and at higher concentration induced formation of massive complexes. No such effects were observed with Mst77F Δ100N, which lacks the region containing the putative coiled coil domain.

We analyzed the impact of Mst77F onto much longer 2432 bp linear DNA, to exclude that the observed effects are uniquely caused by the short 12 bp fragment (Figure 4C). Atomic force microscopy showed at low DNA to protein ratios (1:4) intramolecular DNA bending and local formation of dense ‘hubs’. Higher DNA to protein ratios (1:20) resulted in formation of tightly condensed structures exhibiting multiple interconnected, tightly packed DNA molecules with protruding free fibers. Further increase in protein concentration (1:100) enhanced this condensation effect. In the same experiment the Mst77F Δ100N mutant protein did not have the same DNA condensing properties. The CTD alone formed fibrillar, branched and network-like structures in a concentration-dependent manner. These resembled ‘tram track’-like complexes formed by DNA in complex with histone H1.4 (Supplementary Figure S4B) and might reflect the structural impact of highly charged unstructured domains on DNA (34,35). No effects of Mst77F Δ60C or xPR-Set7 on aggregating DNA were observed in

these assays (Supplementary Figure S4B). The results to this point indicated that the charged CTD of Mst77F mediates unspecific DNA binding, whereas the N-terminal region containing the putative coiled coil domain is required for aggregating DNA.

DNA-binding induces multimerization of Mst77F

To obtain insights into the molecular mechanism of the DNA aggregation effect, we analyzed the multimerization status of the Mst77F protein. Coiled coil motifs are protein interaction domains allowing formation of dimers and higher order assemblies (36). We reasoned that the protein might interact with itself via this region. However, sedimentation velocity analytical ultracentrifugation analysis indicated that Mst77F itself is plainly monomeric (95%) with a small fraction of the protein (5%) representing a dimeric state (Figure 5A).

The strong DNA aggregating effect of Mst77F can hardly be ascribed to the minor dimeric form of the protein. A fundamental feature of unstructured domains is the potential to stably adopt ordered conformations upon interaction with *bona fide* binding partners (37,38). Therefore, we asked whether the conformation of Mst77F upon binding of the CTD to DNA is changed in a manner that possibly induces multimerization. Therefore, we first performed protein-protein cross-linking experiments in the presence of increasing DNA concentrations (Figure 5B). In agree-

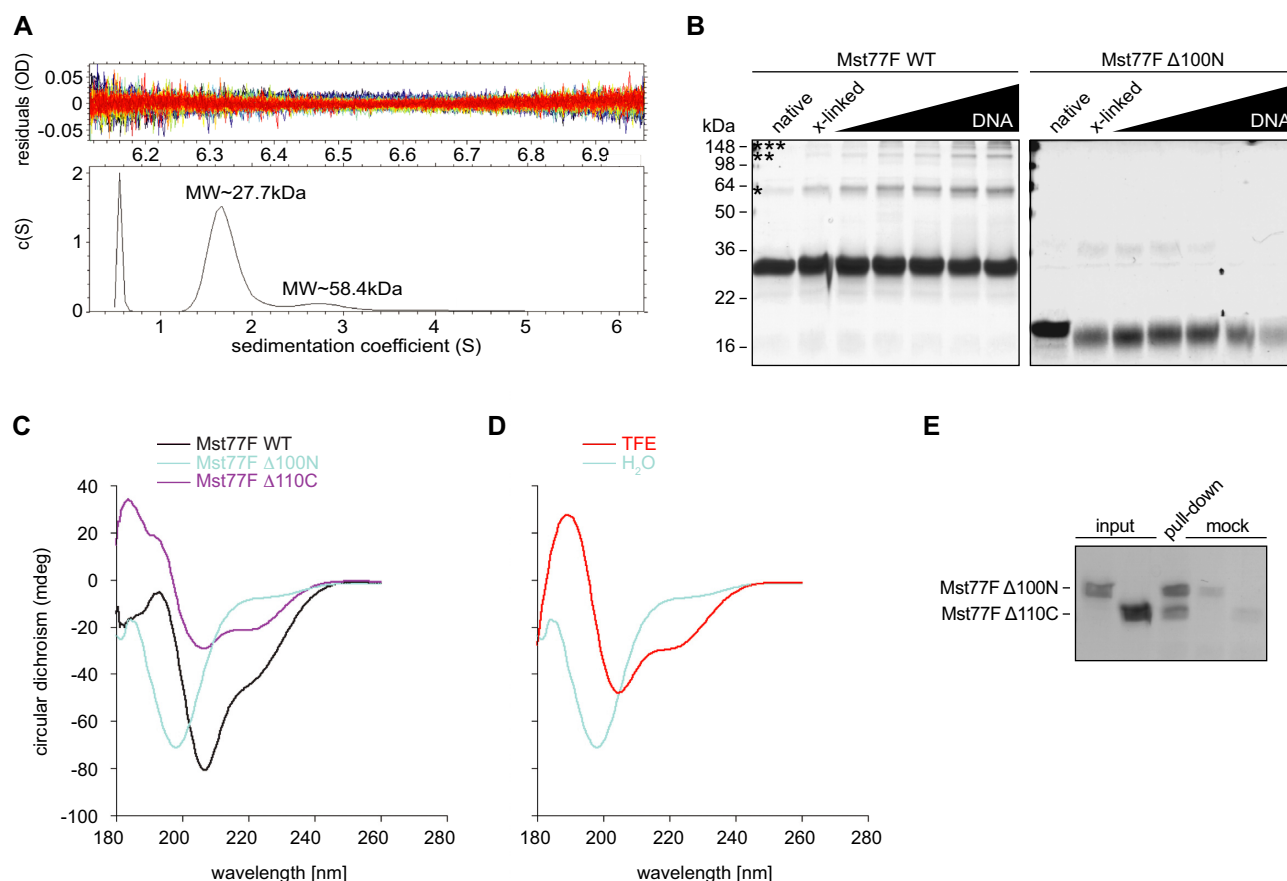


Figure 5. Recognition of DNA induces multimerization of Mst77F. (A) Sedimentation velocity analytical ultracentrifugation of recombinant Mst77F WT. Molecular weights (MW) were calculated from the SEDFIT program by fitting (bottom) the sedimentation raw data (top). Derived protein masses are within the accepted 10% error margin of the method. (B) Cross-linking of Mst77F WT or Mst77F Δ 100N proteins (20 μ M) was carried out with the amine cross linker BS³ in the presence of increasing amounts of DNA (0.3–4.8 pM). Proteins were analyzed on a 15% Tris-glycine SDS-PAGE gel stained with Coomassie Blue. Native, without cross-link; x-linked, cross-linked with BS³. Asterisks indicate dimers (*), tetramers (**) and octamers (***). (C) CD spectroscopy of the indicated proteins under aqueous conditions. (D) Comparison of Mst77F Δ 100N CD spectra under aqueous conditions (H₂O) and in 50% trifluoroethanol (TFE) as secondary structure stabilizing reagent. (E) Biotinylated random 12 bp DNA immobilized on streptavidin-functionalized paramagnetic particles was incubated with Mst77F Δ 100N and Mst77F Δ 110C (pull-down). Proteins recovered on the beads were analyzed by 15% Tris-glycine SDS-PAGE stained with Coomassie Blue. Input, 100%; mock, pull-down using beads only without DNA.

ment with the results of analytical ultracentrifugation, the free form of the protein was monomeric in this assay. Upon addition of DNA to the reaction dose-dependent formation of Mst77F dimers, tetramers and oligomers could be observed. In contrast, the Mst77F Δ 100N mutant did not multimerize under the same conditions. We deduced that the CTD of Mst77F does not interact with itself even in presence of DNA. It might, however, be structurally reorganized/stabilized after binding to DNA thereby mediating protein multimerization via the N-terminus.

To test this idea, we investigated possible induced structural reorganization of the Mst77F CTD using CD far ultraviolet spectroscopy. In agreement with the bioinformatical protein motif and secondary structure predictions, the N-terminal domain displayed a folded conformation in aqueous solution with α -helical content (Figure 5C, purple curve, indicative minima at 208 and 222 nm and maximum at 190 nm). Under the same conditions the CTD essentially showed highly flexible random coil properties. The mean residue molar ellipticity at 222 nm ($[\theta]_{222}$) taken as diagnostic of helix formation was negligible. Nevertheless,

the typical small positive peak at 215 nm characteristic of a pure random coil was not observed suggesting existence of small areas of ordered secondary structure (Figure 5C, turquoise curve). The CD fingerprint of the full-length protein reflected the sum of the individual domain signals with some helical content but overall flexible random coil conformation dominating (Figure 5C, black curve). To imitate the DNA bound state, another CD spectrum of the Mst77F CTD was recorded in presence of 50% trifluoroethanol, which stabilizes secondary structures (39). Indeed, under these conditions an increase in negative ellipticity at 222 and 208 nm as well as appearance of a peak at 190 nm was observed (Figure 5D).

We then analyzed whether CTD and N-terminus of Mst77F could interact in presence of DNA. In pull-down experiments Mst77F Δ 110C by itself did not bind immobilized DNA (Supplementary Figure S3B). However, it could be recovered on the DNA-bound matrix when Mst77F Δ 100N was added (Figure 5E). Since we detected only minor multimerization of Mst77F alone, we deduced from these experiments that DNA binding of the CTD induces

conformational stabilization, which enables this region to interact with the α -helical N-terminus.

Increased Mst77F levels cause chromatin aggregation in sperm

Our *in vitro* experiments indicated that Mst77F interacts with DNA and can multimerize, thereby inducing DNA and chromatin aggregation. Thus, we wanted to analyze Mst77F in *Drosophila* cells and in particular in salivary glands with polytene chromosomes, which allow a high resolution of chromatin. However, we could not establish good expression of Mst77F using the binary UAS/GAL4 (UAS-Mst77F and *sgs4*-GAL4) system (data not shown). This might be due to spermatid specific translational activation or low protein stability (40).

We therefore focused our experiments on spermatogenesis and moderately elevated expression levels. We reasoned that additional copies of *Mst77F-eGFP* (as transgenes under native transcriptional control) in the WT background might interfere with spermiogenesis at the level of chromatin organization. Like endogenous Mst77F we found the Mst77F-eGFP fusion protein expressed under the control of its native promoter and 5' UTR present in sperm chromatin (Figure 6A and C). We analyzed several independent transgenic lines with random integration into the genome bearing different copy numbers (one or two) of *Mst77F-eGFP* either on the second or third chromosome. With two copies of *Mst77F-eGFP* we observed disturbed nuclear morphology in about 20% of spermatids. These spermatids were characterized by aggregated DNA in sperm heads shortly before or during individualization (marked by arrows in Figure 6B and D). We also observed small round nuclei (Figure 6E, arrow head), where DNA and Mst77F-eGFP appeared concentrated in dot-like structures. Flies with three or four additional *Mst77F* genes did not show an enhanced phenotype (see Table 1 for summary of the experiments). We have shown previously that Mst77F-eGFP is biologically functional and the C-terminal eGFP-tag does not interfere with its DNA binding properties, as it can rescue the *Mst77F* mutant phenotype (*ms(3)nc3/DF3L*)*ri-79c*, deletion over a point mutation, same line as used in Figure 6). No aggregated DNA in sperm heads was seen in these flies (16). Thus, deleting one WT *Mst77F* gene copy suppressed the sperm defects. These results indicated that additional copies of *Mst77F-eGFP* in part interfere with the organization of the DNA into a needle shape form of the nucleus likely by causing chromatin aggregation. However, we found only normal sperm in the seminal vesicles (Figure 7B), as we had observed previously for defective spermatid heads in protamine deletion mutants (17). In agreement, one or two additional copies of *Mst77F-eGFP* did not interfere with fertility (Table 1).

We then asked if the chromatin aggregation properties of Mst77F seen in nuclei before and during individualization are dependent on the N-terminal multimerization and the C-terminal DNA interaction domains. We established transgenic *Drosophila* lines expressing Mst77F Δ 20C-eGFP, Mst77F Δ 40C-eGFP, Mst77F Δ 60C-eGFP and Mst77F Δ 100N-eGFP and analyzed males containing two copies of these constructs in addition to the

internal WT genes (Figure 7A and B). Expression of Mst77F Δ 20C-eGFP, which showed *in vitro* DNA-binding similar to the WT protein, caused defects identical to those seen when the full-length fusion protein was overexpressed (Figure 7A and B). Deletion of the C-terminal 40 or 60 amino acids (Mst77F Δ 40C-eGFP, Mst77F Δ 60C-eGFP) caused loss of nuclear localization (data not shown), likely since two NLS are lacking in these constructs (see scheme in Figure 1A and B). Artificial addition of one of both NLS to the C-terminus of Mst77F Δ 40C-eGFP partially restored nuclear localization. Consistent with impaired DNA binding of this mutant protein *in vitro*, no aggregation of chromatin was observed. Importantly, the Mst77F Δ 100N-eGFP mutant lacking the region containing the putative coiled coil region showed nuclear localization but did not cause aggregation (Table 1). The results indicated that both, DNA-binding by the CTD as well as multimerization mediated by the N-terminal region are required for the chromatin aggregation effect of overexpressed Mst77F.

DISCUSSION

Our results shed light on the molecular function of the Mst77F protein and provide new insights into the mechanisms of chromatin organization in sperm development. We provide evidence that Mst77F binds DNA directly via unspecific, electrostatic interaction of its CTD. DNA binding induces multimerization of the protein via the N-terminal domain. As a consequence, free as well as nucleosomal DNA is aggregated and compacted. We think this functionality, first, is important during stepwise reorganization of chromatin in spermiogenesis and, second, directly contributes to the compacted DNA state of *Drosophila* mature sperm.

Mst77F is a unique chromatin architectural protein

We show that Mst77F associates with DNA and chromatin through sequence-unspecific electrostatic interactions of a highly charged CTD with the sugar-phosphate backbone of the nucleic acid. We propose that this region belongs to the growing group of intrinsically unstructured protein domains. Structure prediction algorithms (data not shown) as well as CD analysis fail to detect any secondary structure elements of this region. Intrinsically unstructured domains frequently are involved in macromolecular recognition processes (41,42). These often contain an elevated number of charged residues, which suggests strong electrostatic contributions in binding events (43). Intrinsically disordered domains with high charge density seem to be generally involved in recognition and organization of DNA on a local and genome-wide level. These are present in several proteins that alter chromatin folding and compaction. The CTD of H1 that shows high affinity binding to the nucleosomal linker DNA is a paradigm example (24,44). Also, the HMG-D protein that is associated with condensed chromatin during developmental processes binds unspecifically to DNA, in part via its highly charged, unstructured C-terminus (45,46). Moreover, the repressive function of Polycomb Repressive Complex 1 that compacts chromatin and inhibits remodeling processes relies on one of its subunits

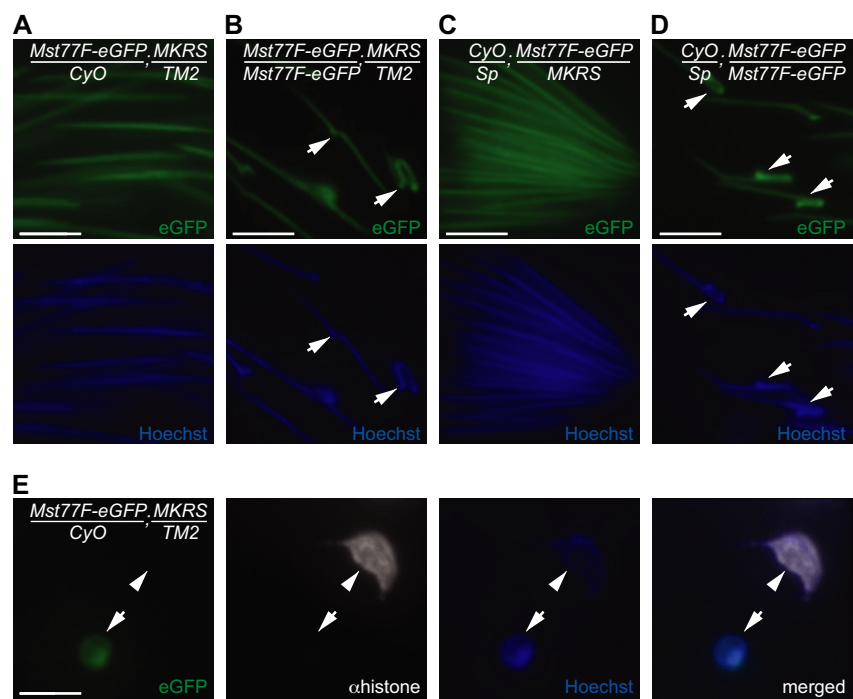


Figure 6. Ectopic expression of Mst77-eGFP during spermiogenesis results in aberrant sperm nuclei. (A–D) Individualizing sperm from males heterozygous (A and C) or homozygous (B and D) for *Mst77F-eGFP* with insertion on the second chromosome (A and B) or on the third chromosome (C and D). Signals for eGFP (top) and DNA stained with Hoechst are shown. Arrows point to deformed nuclei. (E) Representative images of a small round nucleus, which is histone-negative (arrow), and a young elongating nucleus, which is histone-positive (arrow head). Signals for eGFP, core-histones stained with antibodies and DNA labeled with Hoechst are shown. Merged, overlay of the fluorescence signals. Scale bar of all images represents 5 μ m.

Table 1 Summary of *in vitro* and *in vivo* analysis of Mst77F wt and mutant proteins

	<i>in vitro</i>		<i>in vivo</i>		
	DNA binding	DNA aggregation	fertility	nuclear localization	overexpression (wildtype background)
WT (1 copy) 	+++	+++	+	+	homogeneous nuclear distribution of DNA and eGFP signal
WT (2 -4 copies) 	+++	+++	+	+	aggregation of DNA and eGFP signal in areas of the nucleus
Δ 100N (2 copies) 	+++	–	+	+	homogeneous nuclear distribution of DNA and eGFP signal
Δ 20C (2 copies) 	++	nd	+	+	aggregation of DNA and eGFP signal in areas of the nucleus
Δ 40C+NLS (2 copies) 	–	nd	+	+/-	homogeneous nuclear distribution of DNA and eGFP signal; also eGFP signal in cytoplasm
Δ 60C+NLS (2 copies) 	–	–	+	–	no nuclear eGFP signal (data not shown)

NLS: RPRK sequence, indicated by light blue box; nd, not determined.

that interacts with DNA through an intrinsically unstructured, highly charged domain (47). Intrinsically unstructured domains transition from disordered to ordered conformations upon recognition of their respective binding partners (37). Two short, discontinued subdomains within the CTD of histone H1 proteins adopt α -helical structures upon binding to DNA. The formation

of these local secondary structural elements is essential for protein function even though the initial protein-DNA interaction is considered to be purely electrostatic (34,48–49). We propose a similar mode of DNA binding by the CTD of Mst77F, which we think becomes at least partially structured upon DNA-binding. First, we see increased structural organization in stabilizing solvents. Second, the CTD

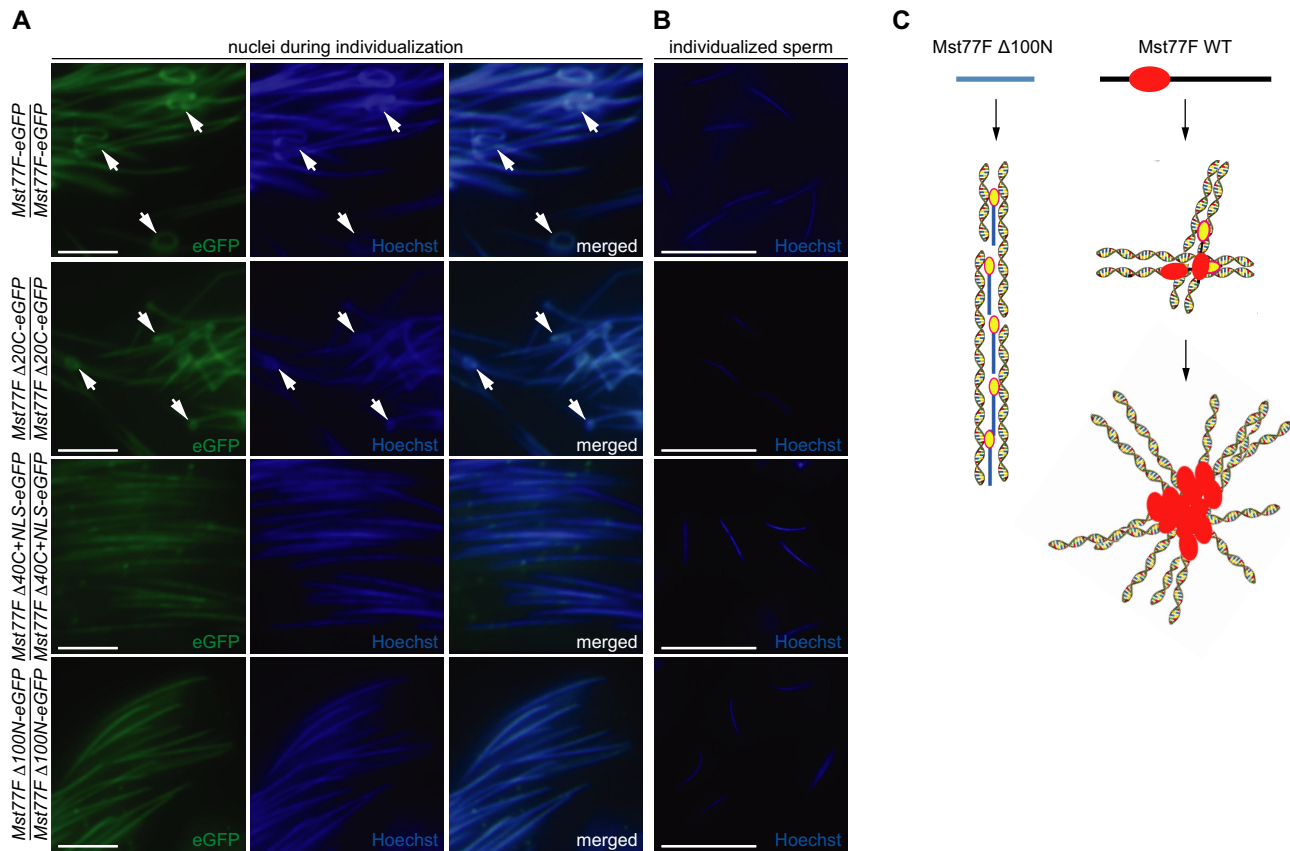


Figure 7. Increased Mst77F levels cause chromatin aggregation. Analysis of testes squash preparations of transgenic flies expressing the indicated WT and mutant Mst77F-eGFP fusion proteins. An artificial NLS sequence was added to the C-terminus of Mst77F $\Delta 40C$. Representative results obtained for five independent strains of each condition with random integration into the genome are shown. (A) Nuclei during individualization. Arrows mark disturbed nuclear morphology of spermatids. DNA was stained with Hoechst. Scale bar represents 20 μm . (B) Nuclei of individualized sperm stained with Hoechst to mark the DNA. Scale bar represents 5 μm . (C) Model of Mst77F function. Mst77F $\Delta 100N$ (blue) unspecifically interacts with DNA, which in turn stabilizes structural motifs in the Mst77F C-terminus (yellow). Since Mst77F $\Delta 100N$ cannot multimerize due to a missing partner interface, this results in aligned DNA molecules that resemble ‘tram track’-like structures. Mst77F WT protein forms homo-multimers through interaction of the N-terminal coiled coil (red) motif with the DNA-induced structures of the C-terminus. Functionally, Mst77F multimerization is guided by cooperativity between the individual molecules resulting in interconnection and compaction of individual Mst77F-bound DNA molecules.

of Mst77F only interacts with the N-terminus when in the DNA-bound state (Figure 5). Since the N-terminus alone has no DNA-binding affinity (Figure 3), this interaction is not mediated via a bridging effect of DNA but indicates structural changes in the CTD.

Communication between the CTD and N-terminus is pivotal for the strong DNA aggregating effect of Mst77F. While the CTD alone has DNA-organizing ability similar to histone H1, the N-terminus is essential for inducing higher order, clustering effects. Since Mst77F in isolation behaves monomeric but forms multimers in presence of DNA, we hypothesize that the DNA-induced interaction of the CTD with this region results in conformational changes that allows protein-protein interaction via the coiled coil motif (36). Alternatively, the partially structured CTD might serve as glue connecting the N-terminal regions of different Mst77F molecules. Since the stabilizing amino acids in the coiled coil are predominantly negatively charged, we think electrostatic repulsion prevents protein multimerization in the free state. The very dense structures observed in atomic force microscopy further sustain a cooperative effect between the CTD and N-terminus of

Mst77F generating a locally very high Mst77F concentration that interconnects individual DNA molecules and restrains their flexibility and motion. In this context the high positive charge density of the CTD might eliminate electrostatic repulsion between neighboring DNA molecules (Figure 7C).

As consequence of the intramolecular crosstalk of the CTD and N-terminus Mst77F can induce massive condensation and aggregation when binding short or longer pieces of DNA. In contrast, H1 has no effect on short pieces of DNA and was shown to align long DNA strands in a parallel, ‘tram track’-like manner (34,35). The globular winged-helix motif of linker histones mediates specific nucleosome positioning, but does not induce chromatin higher order folding (22–23,50). In contrast, Mst77F lacks a globular winged-helix motif but contains a N-terminal coiled coil motif. This predicted domain appears to mediate multimerization but does not function in a targeted nucleosome recognition process. As consequence Mst77F does not bind nucleosomes at the entry/exit point of DNA but associates in a seemingly random way with linker DNA and the surface of the nucleosome (Figure 2) (24).

Function of Mst77F in spermatogenesis

Mst77F is first detectable at the onset of the young elongating nuclei stage, where it is associated with microtubules adjacent to the nucleus and might be involved in nuclear shaping (17). Thereafter, Mst77F enters the nucleus, for which its NLS in the CTD are essential (40). Since histones are present until later stages of spermatid maturation between early and late canoe stage (2), a direct role of Mst77F in evicting histones is unlikely. In agreement, we do not detect such activity *in vitro* (see Figure 2 and data not shown).

Since Mst77F can interact with DNA while associated with histones and as it has severe chromatin aggregation effects, we think the protein might play an important role in initiating chromatin condensation during sperm maturation. Besides, a structural effect that is important for nuclear reshaping, this might be important for shutting down the low level of post-meiotic transcription (15,51,52).

In late post-meiotic spermatids and mature sperm Mst77F is found at distinct spots on the chromatin (17). Since we show sequence unspecific DNA-binding of the protein, other factors must contribute to establishing and maintaining such patterning. Protamines are obviously not involved. Mst77F distribution is not changed in sperm cells of protamine deficient flies (Figure 1B). Since male flies are fertile in the absence of protamines, the major 'default' proteins organizing sperm DNA (17), we think that Mst77F might be sufficient for adequate DNA condensation. Whether Mst77F is causal for DNA condensation in sperm or rather provides a safeguard mechanism in case other systems fail, needs to be analyzed. Additional factors might interplay with Mst77F in this process. Future work will also need to find out whether Mst77F cooperates or competes with protamines in certain functions.

When overexpressed, Mst77F causes aberrant chromatin condensation in developing sperm. The fact that such flies are nevertheless fertile might be caused by the high level of DNA compaction already achieved by protamines. Further compaction might not be possible or have no detrimental effect. Based on the exclusive distribution and its unique DNA architectural properties we hypothesize that Mst77F gives rise to a so far completely unknown condensed chromatin structure.

SUPPLEMENTARY DATA

Supplementary Data are available at NAR Online.

ACKNOWLEDGEMENT

We thank Dr. Samrat Dutta for advice on AFM analysis and Ruth Hyland for help with establishing transgenic *Drosophila* lines.

FUNDING

Max Planck Society [to W.F.]; Marie Curie International Reintegration Fellowship [MIRG-CT-2007-046473 to W.F.]; Deutsche Forschungsgemeinschaft [TRR81 'Chromatin Changes in Differentiation and Malignancies' to R.R.-P.]. Funding for open access charge: Max Planck Society.

Conflict of interest statement. None declared.

REFERENCES

- Chen, C. (2008) *Molecular Mechanisms in Spermatogenesis*. Springer, NY.
- Rathke, C., Baarends, W.M., Awe, S. and Renkawitz-Pohl, R. (2014) Chromatin dynamics during spermiogenesis. *Biochim. Biophys. Acta*, **1839**, 155–168.
- Wouters-Tyrou, D., Martinage, A., Chevaillier, P. and Sautiere, P. (1998) Nuclear basic proteins in spermiogenesis. *Biochimie*, **80**, 117–128.
- Balhorn, R. (2007) The protamine family of sperm nuclear proteins. *Genome Biol.*, **8**, 227.
- Awe, S. and Renkawitz-Pohl, R. (2010) Histone H4 acetylation is essential to proceed from a histone- to a protamine-based chromatin structure in spermatid nuclei of *Drosophila melanogaster*. *Syst. Biol. Reprod. Med.*, **56**, 44–61.
- Dottermusch-Heidel, C., Gartner, S.M., Tegeder, I., Rathke, C., Barckmann, B., Bartkuhn, M., Bhushan, S., Steger, K., Meinhardt, A. and Renkawitz-Pohl, R. (2014) H3K79 methylation: a new conserved mark that accompanies H4 hyperacetylation prior to histone-to-protamine transition in *Drosophila* and rat. *Biol. Open*, **3**, 444–452.
- Dottermusch-Heidel, C., Klaus, E.S., Gonzalez, N.H., Bhushan, S., Meinhardt, A., Bergmann, M., Renkawitz-Pohl, R., Rathke, C. and Steger, K. (2014) H3K79 methylation directly precedes the histone-to-protamine transition in mammalian spermatids and is sensitive to bacterial infections. *Andrology*, **2**, 655–665.
- Gaucher, J., Reynoird, N., Montellier, E., Boussouar, F., Rousseaux, S. and Khochbin, S. (2010) From meiosis to postmeiotic events: the secrets of histone disappearance. *FEBS J.*, **277**, 599–604.
- Tan, M., Luo, H., Lee, S., Jin, F., Yang, J.S., Montellier, E., Buchou, T., Cheng, Z., Rousseaux, S., Rajagopal, N. et al. (2011) Identification of 67 histone marks and histone lysine crotonylation as a new type of histone modification. *Cell*, **146**, 1016–1028.
- Dai, L., Peng, C., Montellier, E., Lu, Z., Chen, Y., Ishii, H., Debernardi, A., Buchou, T., Rousseaux, S., Jin, F. et al. (2014) Lysine 2-hydroxyisobutyrylation is a widely distributed active histone mark. *Nat. Chem. Biol.*, **10**, 365–370.
- Kempisty, B., Jedrzejczak, P. and Jagodzinski, P.P. (2006) [Structure and role of protamines 1 and 2 in spermatogenesis and male infertility]. *Ginekologia polska*, **77**, 238–245.
- Oliva, R. (2006) Protamines and male infertility. *Hum. Reprod. Update*, **12**, 417–435.
- Doyen, C.M., Moshkin, Y.M., Chalkley, G.E., Bezstarosti, K., Demmers, J.A., Rathke, C., Renkawitz-Pohl, R. and Verrijzer, C.P. (2013) Subunits of the histone chaperone CAF1 also mediate assembly of protamine-based chromatin. *Cell Rep.*, **4**, 59–65.
- Gärtner, S.M., Rothenbusch, S., Buxa, M.K., Theofel, I., Renkawitz, R., Rathke, C. and Renkawitz-Pohl, R. (2015) The HMG-box-containing proteins tHMG-1 and tHMG-2 interact during the histone-to-protamine transition in *Drosophila* spermatogenesis. *Eur. J. Cell Biol.*, **94**, 46–59.
- Rathke, C., Baarends, W.M., Jayaramaiah-Raja, S., Bartkuhn, M., Renkawitz, R. and Renkawitz-Pohl, R. (2007) Transition from a nucleosome-based to a protamine-based chromatin configuration during spermiogenesis in *Drosophila*. *J. Cell Sci.*, **120**, 1689–1700.
- Jayaramaiah Raja, S. and Renkawitz-Pohl, R. (2005) Replacement by *Drosophila melanogaster* protamines and Mst77F of histones during chromatin condensation in late spermatids and role of sesame in the removal of these proteins from the male pronucleus. *Mol. Cell. Biol.*, **25**, 6165–6177.
- Rathke, C., Barckmann, B., Burkhard, S., Jayaramaiah-Raja, S., Roote, J. and Renkawitz-Pohl, R. (2010) Distinct functions of Mst77F and protamines in nuclear shaping and chromatin condensation during *Drosophila* spermiogenesis. *Eur. J. Cell Biol.*, **89**, 326–338.
- Iguchi, N., Tanaka, H., Yomogida, K. and Nishimune, Y. (2003) Isolation and characterization of a novel cDNA encoding a DNA-binding protein (Hils1) specifically expressed in testicular haploid germ cells. *Int. J. Androl.*, **26**, 354–365.
- Yan, W., Ma, L., Burns, K.H. and Matzuk, M.M. (2003) HILS1 is a spermatid-specific linker histone H1-like protein implicated in

- chromatin remodeling during mammalian spermiogenesis. *Proc. Natl. Acad. Sci. U.S.A.*, **100**, 10546–10551.
20. Bryant, J.M., Govin, J., Zhang, L., Donahue, G., Pugh, B.F. and Berger, S.L. (2012) The linker histone plays a dual role during gametogenesis in *Saccharomyces cerevisiae*. *Mol. Cell. Biol.*, **32**, 2771–2783.
 21. Russell, S.R. and Kaiser, K. (1993) *Drosophila melanogaster* male germ line-specific transcripts with autosomal and Y-linked genes. *Genetics*, **134**, 293–308.
 22. McBryant, S.J., Lu, X. and Hansen, J.C. (2010) Multifunctionality of the linker histones: an emerging role for protein-protein interactions. *Cell Res.*, **20**, 519–528.
 23. Happel, N. and Doenecke, D. (2009) Histone H1 and its isoforms: contribution to chromatin structure and function. *Gene*, **431**, 1–12.
 24. Allan, J., Hartman, P.G., Crane-Robinson, C. and Aviles, F.X. (1980) The structure of histone H1 and its location in chromatin. *Nature*, **288**, 675–679.
 25. Caterino, T.L. and Hayes, J.J. (2011) Structure of the H1 C-terminal domain and function in chromatin condensation. *Biochem. Cell Biol.*, **89**, 35–44.
 26. Christophorou, M.A., Castelo-Branco, G., Halley-Stott, R.P., Oliveira, C.S., Loos, R., Radziszewska, A., Mowen, K.A., Bertone, P., Silva, J.C., Zernicka-Goetz, M. *et al.* (2014) Citrullination regulates pluripotency and histone H1 binding to chromatin. *Nature*, **507**, 104–108.
 27. Jacobs, S.A., Fischle, W. and Khorasanizadeh, S. (2004) Assays for the determination of structure and dynamics of the interaction of the chromodomain with histone peptides. *Methods Enzymol.*, **376**, 131–148.
 28. Schwarz, P.M., Felthaus, A., Fletcher, T.M. and Hansen, J.C. (1996) Reversible oligonucleosome self-association: dependence on divalent cations and core histone tail domains. *Biochemistry*, **35**, 4009–4015.
 29. Schuck, P. (2000) Size-distribution analysis of macromolecules by sedimentation velocity ultracentrifugation and lamm equation modeling. *Biophys. J.*, **78**, 1606–1619.
 30. Thummel, C.S., Boulet, A.M. and Lipshitz, H.D. (1988) Vectors for *Drosophila* P-element-mediated transformation and tissue culture transfection. *Gene*, **74**, 445–456.
 31. Michiels, F., Buttgeriet, D. and Renkawitz-Pohl, R. (1993) An 18-bp element in the 5' untranslated region of the *Drosophila* beta 2 tubulin mRNA regulates the mRNA level during postmeiotic stages of spermatogenesis. *Eur. J. Cell Biol.*, **62**, 66–74.
 32. Huynh, V.A., Robinson, P.J. and Rhodes, D. (2005) A method for the in vitro reconstitution of a defined '30 nm' chromatin fibre containing stoichiometric amounts of the linker histone. *J. Mol. Biol.*, **345**, 957–968.
 33. Brown, D.T., Izard, T. and Misteli, T. (2006) Mapping the interaction surface of linker histone H1(0) with the nucleosome of native chromatin in vivo. *Nat. Struct. Mol. Biol.*, **13**, 250–255.
 34. Lu, X., Hamkalo, B., Parseghian, M.H. and Hansen, J.C. (2009) Chromatin condensing functions of the linker histone C-terminal domain are mediated by specific amino acid composition and intrinsic protein disorder. *Biochemistry*, **48**, 164–172.
 35. Lucius, H., Haberland, A., Zaitsev, S., Dalluge, R., Schneider, M. and Bottger, M. (2001) Structure of transfection-active histone H1/DNA complexes. *Mol. Biol. Rep.*, **28**, 157–165.
 36. Mason, J.M. and Arndt, K.M. (2004) Coiled coil domains: stability, specificity, and biological implications. *ChemBiochem*, **5**, 170–176.
 37. Uversky, V.N. (2002) Natively unfolded proteins: a point where biology waits for physics. *Protein Sci.*, **11**, 739–756.
 38. Tompa, P. (2002) Intrinsically unstructured proteins. *Trends Biochem. Sci.*, **27**, 527–533.
 39. Sonnichsen, F.D., Van Eyk, J.E., Hodges, R.S. and Sykes, B.D. (1992) Effect of trifluoroethanol on protein secondary structure: an NMR and CD study using a synthetic actin peptide. *Biochemistry*, **31**, 8790–8798.
 40. Barckmann, B., Chen, X., Kaiser, S., Jayaramaiah-Raja, S., Rathke, C., Dottermusch-Heidel, C., Fuller, M.T. and Renkawitz-Pohl, R. (2013) Three levels of regulation lead to protamine and Mst77F expression in *Drosophila*. *Dev. Biol.*, **377**, 33–45.
 41. Dunker, A.K. and Obradovic, Z. (2001) The protein trinity—linking function and disorder. *Nat. Biotechnol.*, **19**, 805–806.
 42. Hansen, J.C., Lu, X., Ross, E.D. and Woody, R.W. (2006) Intrinsic protein disorder, amino acid composition, and histone terminal domains. *J. Biol. Chem.*, **281**, 1853–1856.
 43. Vucetic, S., Brown, C.J., Dunker, A.K. and Obradovic, Z. (2003) Flavors of protein disorder. *Proteins*, **52**, 573–584.
 44. Fang, H., Clark, D.J. and Hayes, J.J. (2012) DNA and nucleosomes direct distinct folding of a linker histone H1 C-terminal domain. *Nucleic Acids Res.*, **40**, 1475–1484.
 45. Dow, L.K., Jones, D.N., Wolfe, S.A., Verdine, G.L. and Churchill, M.E. (2000) Structural studies of the high mobility group globular domain and basic tail of HMG-D bound to disulfide cross-linked DNA. *Biochemistry*, **39**, 9725–9736.
 46. Ner, S.S., Blank, T., Perez-Paralle, M.L., Grigliatti, T.A., Becker, P.B. and Travers, A.A. (2001) HMG-D and histone H1 interplay during chromatin assembly and early embryogenesis. *J. Biol. Chem.*, **276**, 37569–37576.
 47. Beh, L.Y., Colwell, L.J. and Francis, N.J. (2012) A core subunit of Polycomb repressive complex 1 is broadly conserved in function but not primary sequence. *Proc. Natl. Acad. Sci. U.S.A.*, **109**, E1063–E1071.
 48. Lu, X. and Hansen, J.C. (2004) Identification of specific functional subdomains within the linker histone H10 C-terminal domain. *J. Biol. Chem.*, **279**, 8701–8707.
 49. Vila, R., Ponte, I., Jimenez, M.A., Rico, M. and Suau, P. (2002) An inducible helix-Gly-Gly-helix motif in the N-terminal domain of histone H1e: a CD and NMR study. *Protein Sci.*, **11**, 214–220.
 50. Woodcock, C.L., Skoultchi, A.I. and Fan, Y. (2006) Role of linker histone in chromatin structure and function: H1 stoichiometry and nucleosome repeat length. *Chromosome Res.*, **14**, 17–25.
 51. Barreau, C., Benson, E., Gudmannsdottir, E., Newton, F. and White-Cooper, H. (2008) Post-meiotic transcription in *Drosophila* testes. *Development*, **135**, 1897–1902.
 52. Vrbancovski, M.D., Chalopin, D.S., Lopes, H.F., Long, M. and Karr, T.L. (2010) Direct evidence for postmeiotic transcription during *Drosophila melanogaster* spermatogenesis. *Genetics*, **186**, 431–433.